Irreversibility line of Bi2223/Ag tape in high magnetic fields

Kušević, Ivica; Babić, Emil; Cooper, John R.; Wang, Wei Guo; Liu, Hua Kun; Dou, Shi Xue

Source / Izvornik: **Fizika A, 1999, 8, 319 - 332**

Journal article, Published version
Rad u časopisu, Objavljena verzija rada (izdavačev PDF)

Permanent link / Trajna poveznica: https://urn.nsk.hr/urn:nbn:hr:217:901772

ISSN 1330–0008
CODEN FIZAE4

IRREVERSIBILITY LINE OF Bi2223/Ag TAPE IN HIGH MAGNETIC FIELDS

IVICA KUŠEVIĆ[a], EMIL BABIĆ[a], JOHN R. COOPER[b], WEI GUO WANG[c], HUA KUN LIU[c] and SHI XUE DOU[c]

[a] *Department of Physics, Faculty of Science, University of Zagreb, 10000 Zagreb, Croatia*

[b] *Interdisciplinary Research Centre in Superconductivity, University of Cambridge, Madingley Road, Cambridge CB3 OHE, United Kingdom*

[c] *Centre for Superconducting and Electronic Materials, University of Wollongong, Wollongong, NSW 2522, Australia*

Dedicated to Professor Boran Leontić on the occasion of his 70$^{\mathbf{th}}$ birthday

Received 23 November 1999; Accepted 10 April 2000

The magnetoresistance of a $(Bi,Pb)_2Sr_2Ca_2Cu_3O_{10+y}$ Ag sheathed tape was measured in the temperature range 15 K $\leq T \leq$ 120 K and magnetic field $B \leq$ 15 T applied perpendicular to the broader surface of tape. Throughout the explored field range, the onset of resistivity shows Arrhenius behaviour $\rho \propto \exp(-U^*(1 - T/T_{cs})/k_B T B^{0.5})$ where U^* is the sample dependent constant, and T_{cs} is the temperature somewhat higher than the temperature of the resistivity onset. The observed resistance variation can be attributed to a thermally activated flux flow in a highly viscous vortex-liquid regime characterized by a plastic deformation of vortices. Experimentally determined resistive irreversibility line B_{irr} vs. T_{irr} follows the power-law dependence $B_{irr}(T_{irr}) \propto (T_{cs}/T_{irr} - 1)^2$ which can be derived from the exponential behaviour of resistivity. Our $B_{irr}(T_{irr})$ data can also be fitted by the combination of the Josephson coupling model and depinning of pancake vortices. This fit provides very reasonable values for B_{c2}, B_{c1}, B_c, ξ_{ab} and λ_{ab} of Bi2223 compound, and removes the unphysical divergence of $B_{irr}(T \to 0)$ resulting from the above power-law fit.

PACS numbers: 74.25.Fy, 74.60.Ge, 74.72.Hs UDC 538.945

Keywords: $(Bi,Pb)_2Sr_2Ca_2Cu_3O_{10+y}$Ag sheathed tape, magnetoresistance, viscous vortex-liquid regime, resistive irreversibility line

1. Introduction

The analysis of dissipation in the mixed state of high-temperature superconductors (HTS) is very important for understanding flux dynamics and related

applications. Such analysis provides detailed understanding of conventional low-temperature type II superconductors [1] (LTS), but in HTS, based on copper oxide, the situation is much more complicated because of their high critical temperatures (T_c) and pronounced anisotropy [2]. Accordingly, the magnetic field vs. temperature (B-T) phase diagrams for HTS are much more complex [2] than those for LTS. One common feature of these diagrams for HTS is the irreversibility line $B_{\rm irr}(T)$ situated well below the upper critical field line $B_{c2}(T)$ over most of the B-T plane [2]. Since $B_{\rm irr}(T)$ separates the magnetically irreversible (finite critical current density J_c) from magnetically reversible regime ($J_c = 0$), it is particularly important for the understanding of flux dynamics in HTS. The results obtained on HTS single crystals suggest that the layered structure has most important effects on the dissipation in HTS [3, 4] and, accordingly, it has been concluded that in highly anisotropic HTS (such as Bi-Sr-Ca-Cu-O compounds), the pinning centers (crucial for practical applications of LTS) only play a minor role [3]. This conclusion is supported by the short coherence lengths in HTS and the presence of Josephson's vortices in highly anisotropic superconductors [5]. However this conclusion was undermined by the introduction of small quantities of impurities, defects (e.g. by irradiation) or twin boundaries in Y-Ba-Cu-O samples, because they proved to be an efficient way for enhancing their extrinsic properties [6] (such as J_c). This suggests that, in addition to the parameters associated with the layered structure of a given compound, flux dynamics in HTS depends on the pinning centers associated with the method of sample preparation and processing.

In this paper we report the results of electrical resistivity (ρ) measurements on a highly-textured Ag-sheathed $(Bi,Pb)_2Sr_2Ca_2Cu_3O_{10+y}$ (hereafter Bi2223) tape in magnetic fields up to 15 T. The low resistivity part of $\rho(T, B)$ dependence shows Arrhenius behaviour indicating that the pinning can be characterized by an effective activation energy $U(T, B)$. We determined the irreversibility line (IL) using a constant-resistivity criterion. The $B_{\rm irr}(T)$ variation for our tape is discussed in terms of the models which are most frequently employed in explaining the dissipation in Bi-Sr-Ca-Cu-O superconductors. Finally, we compare our results for $B_{\rm irr}(T)$ with those for the Bi2212 single crystals [7] measured up to 50 T.

2. Experimental

The Ag-sheathed Bi2223 tape was prepared [8] by the conventional powder-in-tube technique. The nominal chemical composition of the Bi2223 sample was $Bi_{1.84}Pb_{0.34}Sr_{1.91}Ca_{2.03}Cu_{3.06}O_x$, and additional details of preparation have been published previously [8]. For the measurements reported here, short samples of length 1.5 cm were cut from the fully treated tape, which was 4 mm wide. The core cross-sectional area was determined with an optical imaging analyzer. Powder X-ray diffraction analysis of the core showed approximately 15% of the Bi2212 phase [8]. The Bi2223/Ag tape employed in the present experiments was from the same batch as the tape used in Ref. [9].

A standard four-contact method was employed for the AC resistance measurements. All wires were soldered onto the Ag sheath with Wood's alloy to minimize

contact resistances. The applied frequency was 18.4 Hz and the RMS current ranged from 1 – 3 mA (the corresponding current densities were 2.5 – 7.5 A/cm^2 using the core cross-section of the Bi2223/Ag tape). Additional measurements were made at the International Research Centre in Superconductivity (IRCS) (Cambridge) using a frequency of 75.5 Hz and a maximum magnetic field of 15 T. The temperatures were monitored by a carbon-glass resistor (Cambridge) or with an AuFe-Chromel thermocouple (Zagreb). The field was always applied above T_c and perpendicular to the direction of current and to the broader surface of the tape (parallel to the average c-axis of grains). The cooling rate was 0.2 – 0.4 K/min. The critical current density J_c(77 K, self-field) determined with a 1 μV/cm criterion was 30000 A/cm^2. Some data relevant to our sample are given in Table 1.

TABLE 1. Some data for our Bi2223/Ag *sample: A is the bare superconducting cross-section, J_c is the critical current density at $T = 77$ K and $B = 0$, T_{c0} is the critical temperature defined as $R(T = T_{c0}, B = 0) = 0$, and U^*/k_B, α, ρ^* and T_{cs} are fitting parameters (defined in the text) derived from the Arrhenius behaviour of the resistivity onset for $B \leq 15$ T.*

A 10^{-4} cm^2	J_c A/cm^2	T_{c0} K	U^*/k_B KT$^\alpha$	α	ρ^* mΩcm	T_{cs} K
2.76	30000	106.4	2260±70	0.50±0.02	4.5±2.0	118±6

3. Results

Figure 1 is an example of resistive transitions $R(T, B)$ for Bi2223/Ag ($0 \leq B \leq 15$ T) sample. As discussed elsewhere [10], our sample is a composite system of a superconducting core within a silver sheath, therefore the measured resistance is the resistance of a parallel combination of these two "resistors". Since the resistance above T_c is practically the resistance of silver, which is much lower than the resistance of the core, reliable analysis is possible only in the low-resistance part of the $R(T, B)$ curves where the resistance of the core is much lower than that of the Ag-sheathing. Therefore the typical $R(T, B)$ dependencies of corresponding single systems (Bi2223 epitaxial thin films, for example [11]), differ from ours in the high-resistivity region (above approximately 20 nΩcm). The numerical values of the electrical resistivity $\rho(T, B)$, shown in Fig. 1, were obtained by using the superconducting core cross-sectional area.

The inset to Fig. 1 shows Arrhenius plots of $\rho(T, B)$ dependencies for our Bi2223/Ag sample. From these plots, the linear behaviour of $\ln \rho$ vs. $1/T$ is clearly visible, giving the resistivity

$$\rho(T, B) = \rho_0 \exp\left(\frac{-U(T, B)}{k_B T}\right) \tag{1}$$

where $U(T, B)$ is an effective activation energy and k_B is Boltzmann's constant. The lower limit $\rho_l \approx 0.2$ nΩcm of the Arrhenius behaviour is given by our experimental sensitivity, while the upper limit ρ_u is strongly affected by the resistivity of silver.

As shown elsewhere [10], the subtraction of the resistance due to Ag-sheathing increases ρ_u. However, if we limit our analysis just to the measured raw data and from the typical normal state resistivity data $\rho_n \approx 200\ \mu\ \Omega$cm in the normal region just above T_c (the actual value of ρ_n depending somewhat on the type of samples [11–13]), then for our Bi2223/Ag sample $\rho_u \approx 5.6$ nΩcm (which gives the thermally activated resistance range from $10^{-6}\rho_n$ to $2.8 \times 10^{-5}\rho_n$). Also, since the resistivity of silver is strongly field dependent [14] for $B > 1$ T and $T < 50$ K, that range is preserved despite the lowering the overall resistance for $T < 50$ K (Fig. 1).

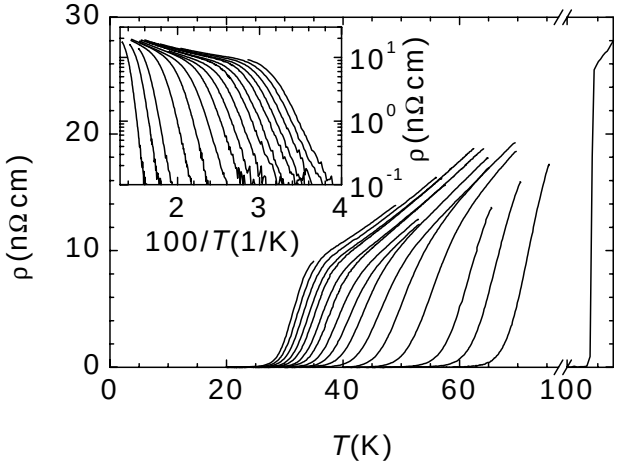

Fig. 1. Resistive transitions in $B = 0$, 1, 1.5, 2, 3, 4, 5, 6, 7, 8, 9, 10, 11, 12, 13, 14 and 15 T *(right to left) for the* Bi2223/Ag *tape. The inset: Arrhenius plot of the $\rho(T, B)$ dependence for the same fields without $B = 0$ (left to right).*

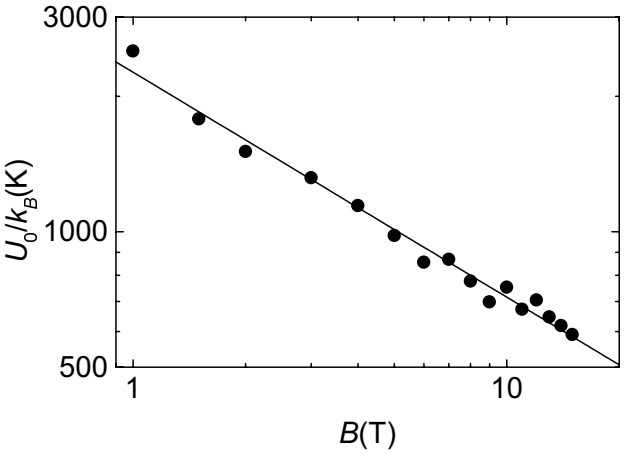

Fig. 2. Dependence of the pinning potential U_0/k_{B} vs. B for $1 \leq B \leq 15$ T *of the* Bi2223/Ag *tape. Line represents the corresponding least squares fit of $U_0/k_{\mathrm{B}} \propto B^{-\alpha}$ with the obtained exponent $\alpha = 0.50 \pm 0.02$.*

Fitting the linear parts of $\ln \rho(T,B)$ by Eq. (1) gives the magnetic field-dependent parameters ρ_0 and $U_0 \equiv U(T=0,B)$. In order to show their dependence on field, two plots are given: log-log plot of U_0 vs. B (Fig. 2) and ρ_0 vs. U_0 (inset to Fig. 3). From the linear dependence in Fig. 2, we see that $U_0(B) = U^*/B^\alpha$, where $\alpha = 0.50 \pm 0.02$ and $U^*/k_\mathrm{B} = 2260$ KT$^\alpha$ is equal to the value of the pinning potential in degrees Kelvin at $B = 1$ T (see also Table 1).

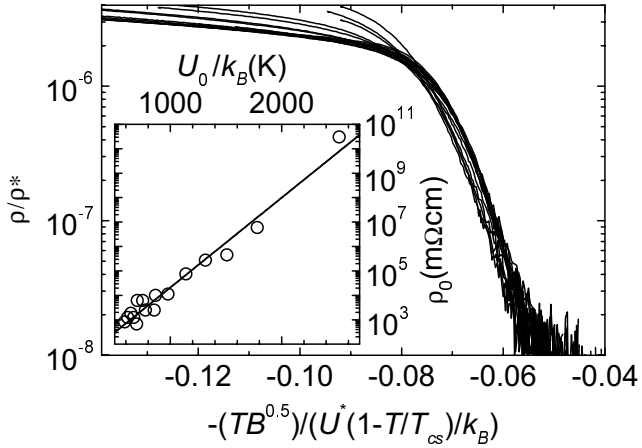

Fig. 3. Scaling of the core resistivity using the fitting parameters $U^*/k_\mathrm{B} = 2260$ KT$^{0.5}$ and $T_\mathrm{cs} = 118$ K for $1 \le B \le 15$ T. The inset: plot showing exponential dependence of the prefactor ρ_0 (Eq. (1)) vs. U_0/k_B for $1 \le B \le 15$ T. Line represents the least square fit $\rho_0 = \rho^* \exp(U_0/k_\mathrm{B}T_\mathrm{cs})$ with $\rho^* = 4.5$ mΩcm and $T_\mathrm{cs} = 118$ K.

The inset to Fig. 3 shows that ρ_0 depends exponentially on U_0 and, therefore, $\rho_0 = \rho^* \exp(U_0/k_\mathrm{B}T_\mathrm{cs})$, where the fitting parameters ρ^* and T_cs are given in Table 1. Within experimental error, T_cs is equal to 118 K, i.e. about 12 K higher than $T_{c0} = T(R=0,B=0)$.

From two above-mentioned dependencies, we can write the unified relation

$$\rho(T,B) = \rho^* \exp\left(-\frac{U^*}{k_\mathrm{B}TB^\alpha}\left(1-\frac{T}{T_\mathrm{cs}}\right)\right) \tag{2}$$

where $\alpha = 0.5$ and $T_\mathrm{cs} = 118$ K. According to Eq. (2), the low-resistance parts of all our $\rho(T,B)$ curves can be scaled onto a single curve by plotting ρ/ρ^* vs. $-TB^{0.5}/(U^*(1-T/T_\mathrm{cs})/k_\mathrm{B})$, which is shown in Fig. 3 for $1 \le B \le 15$ T. A similar analysis performed for the epitaxial Bi2223 films [12] and Bi2212 thin films [15] also yielded higher (≈ 10 K) T_cs values than T_{c0} ones.

From $\rho(T,B)$ measurements, we can define the "resistive" irreversibility line (IL) $B_\mathrm{irr} - T_\mathrm{irr}$ using the constant-resistivity criterion ρ_{cr}. In our case, the lowest experimentally reliable values of the ρ_{cr} were 0.2 nΩcm, therefore the fraction f of the assumed normal state core resistivity $\rho_n = 200$ μΩcm is 10^{-6}. The obtained IL for 1 – 15 T is given in Fig. 4.

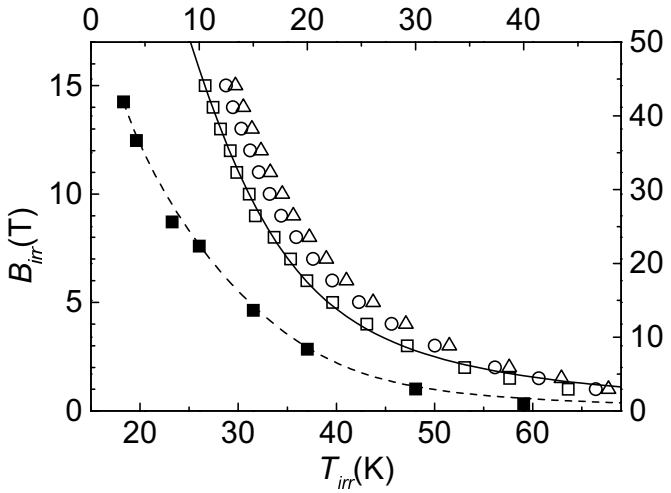

Fig. 4. Irreversibility line $B_{\rm irr}$ vs. $T_{\rm irr}$ for Bi2223/Ag *tape in* $1 \leq B \leq 15$ T *for* $f = 10^{-6}$ *(□),* 5×10^{-6} *(○) and* 10^{-5} *(Δ). The irreversibility line of a* Bi2212 *single crystal from Ref. 7 (full squares) is shown for comparison (top and right scales). Solid and dashed lines represent fits to Eq. (9) (see text).*

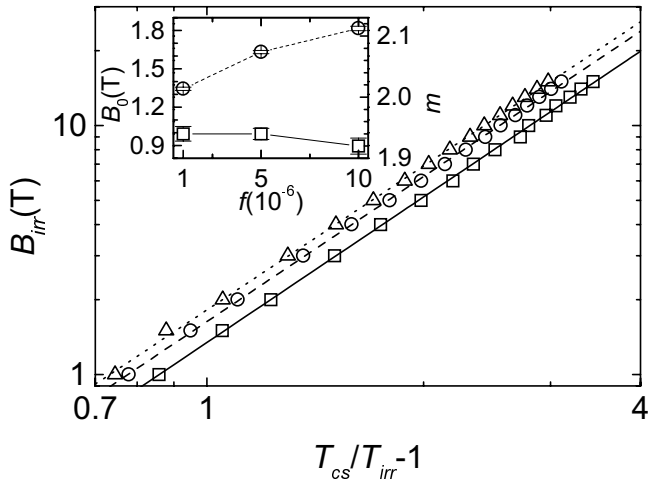

Fig. 5. $B_{\rm irr}$ vs. $(T_{\rm cs}/T_{\rm irr} - 1)$ dependences in the log–log plot that follows Eq. (4) for $1 \leq B \leq 15$ T *for* $f = 10^{-6}$ *(□),* 5×10^{-6} *(○) and* 10^{-5} *(Δ). Lines represent the corresponding least squares fit of experimental data to Eq. (4). The inset: variation of the parameters of the fit to Eq. (4) with f* ($B_0 - ○$, $m - □$).

Quantitative behaviour of the IL can be obtained from Eq. (2), by inserting

$f\rho_n$ instead of ρ, yielding

$$B_{\rm irr}(T_{\rm irr}) = \left(-\frac{U^*}{k_{\rm B}T_{\rm cs}\ln(f\rho_n/\rho^*)}\right)^{1/\alpha}\left(\frac{T_{\rm cs}}{T_{\rm irr}}-1\right)^{1/\alpha}. \qquad (3)$$

Therefore, we can approximate experimentally the obtained IL by the expression

$$B_{\rm irr}(T_{\rm irr}) = B_0(T_{\rm cs}/T_{\rm irr}-1)^m, \qquad (4)$$

and compare the values of B_0 and m from Eq. (4) (obtained from the linear regression $\ln B_{\rm irr}$ vs. $\ln(T_{\rm cs}/T_{\rm irr}-1)$, Fig. 5), with the prefactor in Eq. (3) and exponent $1/\alpha$. Furthermore, since the experimentally obtained IL (and also the prefactor in Eq. (4)) depends on f, we performed the above-mentioned analysis for three different values of f. The parameters B_0 and m are plotted vs. f in the inset to Fig. 5. It is seen that the values of B_0 increase with f, which is expected because $f\rho_n = \rho_{cr}$ rises. Values of m slightly lower in f, but they are approximately equal to 2, which is consistent with $1/\alpha \approx 2$.

4. Discussion

IL is usually determined from magnetic measurements and it divides $B-T$ phase diagram of HTS into two regions, that below the IL showing irreversible magnetic behaviour originating in the pinned vortex lattice or glass, and above the IL the reversible magnetic behaviour attributed to a vortex liquid [2]. In other words, IL is associated with the onset of dissipation in HTS. Often the IL is claimed to be the vortex liquid-vortex glass transition line (melting), decoupling line or depinning line, and all that ambiguity is further complicated by the degree of anisotropy of different compounds. On the other hand, IL is also important from the practical point of view, the region below IL being useful for technical applications of HTS. Therefore, it is desirable to know its functional dependence, which in our case is given by Eq. (4) for $T \geq 26$ K. Since our IL is determined from the Arrhenius-like part of resistance (we were limited by the sensitivity of the experimental arrangement,
approx 0.2 nV), we cannot state that our IL is associated with either of the mechanisms mentioned above. (Note that Eq. (1) yields finite resistance at all temperatures other than $T = 0$ K.) However, it is worthwhile to compare our observed IL dependence (following Eq. (4)) to dependencies observed for other HTS samples.

Usually the melting line of pure HTS single crystals is well approximated by [2] $B_m = B_{m0}(1-T/T_c)^n$ for $T \to T_c$, and exponent n (depending on compound) varies between 1 and 2.4 [16–19], but at lower temperatures, as in our case, such dependence is not likely to appear. For a Bi2212 single crystal, Schilling et al. [20] obtained the same dependence of IL as our one (given by Eq. (4) with $m \approx 2$) which, in their case, coincides with the melting line deduced from the magnetic measurements using a SQUID probe, but only for $T \to T_c$ and $B \ll B_{cr}$ ($B_{cr} \approx$

$4\Phi_0/s^2\gamma^2$ denotes a crossover field from a 3D to a quasi-2D vortex fluctuations [21, 22], where s is the spacing between two CuO_2 planes and $\gamma = (m_c/m_{ab})^{1/2}$ is the anisotropy parameter). Depending on γ, B_{cr} is typically below 1 T for Bi2212, so Eq. (4) fits their data above 55 K and for $B < 0.1$ T, while we have a reverse case - Eq. (4) fits our data over the whole explored range 1 – 15 T. The power-law dependence of IL, also determined resistively and analogous to Eq. (4) with $m = 2$, has been observed on Bi2223 epitaxial films [12] for fields up to 12 T and the authors attribute its origin to plastic deformation of flux lines (we discuss this mechanism below). A recent study [11] of $\rho(T, B)$ in Bi2223 films for $B \leq 6$ T reported departures from an Arrhenius behaviour (AB) in the tail of $\rho(T)$ curves, and that the resistivity followed the vortex-glass (VG) scaling law [2] $\rho \propto (T - T_g)^n$, where T_g is the proposed VG transition temperature and n is the critical exponent. The VG-liquid transition line $B_g(T_g)$ obeyed Eq. (4) with $m = 2$ and $B_0 \simeq 0.6$ T. Since for $B > 1$ T the temperatures $T^*(B)$ for the onset of AB were approximately proportional to $T_g(B)$, they probably obey Eq. (4), too (but with a higher prefactor B_0). Therefore, the results in Ref. [11] indicate the same variation of IL, irrespective whether it is deduced from VG scaling law or from AB at fixed ρ_{cr}.

On the other hand, $B_g(T_g)$ line deduced from the scaling of $I - V$ curves in Bi2223/Ag tapes [23] lies below our IL in a qualitative agreement with the above discussion. However, since in Bi2223/Ag tapes U_0 (and IL) depend on the composition, preparation and processing [24], the quantitative comparison between $B_g(T_g)$ and IL(AB) should be performed on the same sample.

Now, we briefly discuss a possible origin of the Arrhenius behaviour of the resistance given by Eq. (1). Comparison of our data with those obtained on epitaxial Bi2223 film [11] and Bi2223/Ag tapes [23] indicates that we are above the so-called VG transition, in agreement with the fact that our resistivities are independent of the measuring current, i.e. according to the standard interpretation we are in the vortex – liquid region of the phase diagram. According to the theory of Geshkenbein et al. [25], the vortex liquid is highly viscous and the characteristic activation energy corresponds to the energy of a double-kink (length $2a$) in a line vortex, therefore, using anisotropic Ginzburg-Landau theory, the double kink energy is

$$U = \frac{\Phi_0^2 a}{4\pi\mu_0(\lambda_{ab}\lambda_c)^2} \ln\left(\frac{\lambda_{ab}\lambda_c}{\xi_{ab}\xi_c}\right)^{1/2} \tag{5}$$

where Φ_0 is the flux quantum, $a \approx (\Phi_0/B)^{1/2}$ is the intervortex spacing, and λ_{ab}, λ_c, ξ_{ab} and ξ_c are penetration depths and correlation lengths in the a–b plane or c–axis direction. From Eq. (5) follow the temperature $(1 - T/T_c)$ and field $(B^{-0.5})$ dependencies of U, which are in agreement with the form of our derived activation energy (Eq. (2)). Similar behaviour has been observed in Bi2212 films [15, 26], Bi2212 crystals [27, 28], Bi2223 films [11, 12] and whiskers [29], and YBCO crystals (from the resistance [30], relaxation of the magnetization [31] and $I - V$ curves [32], but with $\alpha \approx 0.3 - 0.7$ for different field ranges, see original references). We emphasize that Ref. [28] reported $U(T, B)$ variation consistent with Eq. (5) for $B \leq 18$ T and that Eq. (5) yields $U^*(\gamma, \lambda_{ab})$ values comparable to those observed

[15]. On the other hand, the magnitudes of activation energy are very sensitive to the class of the samples and the typical values of $U_0(1\ \mathrm{T})/k_\mathrm{B}$ for Bi2212 crystals are 600 K, 1000–2000 K for Bi2212 films and 1300–2000 K for Bi2223 films and whisker. Our value of $U_0(1\ \mathrm{T})/k_\mathrm{B} = 2520$ K belongs to the upper class of the activation energy values. Another parameter, which directly influences the U_0 values in Bi2223 tapes, is the content of Bi2212 phase, showing that in well-prepared tapes and for low fraction of Bi2212 phase (less than approximately 10%), $U_0(1\ \mathrm{T})/k_\mathrm{B}$ can reach 5000 K [24]. Therefore, we can conclude that in the presence of uncorrelated disorder (increasing in the order crystal–film–tape) which gives stronger pinning, the activation energy rises in the same manner as the degree of disorder. The effects of such disorder may possibly be incorporated into the Geshkenbein's model as a restriction on the formation of double kinks and, therefore, may affect U_0 but not the form of $U(T, B)$ given in Eq. (5). Finally, we note that the entanglement of the flux lines [2] may provide a similar magnitude and variation of $U(T, B)$ as the above mechanism.

However, both the plastic deformation and entanglement rely on the existence of 3D flux lines which is not likely above B_{cr}, and this presents the main problem for the explanation of U_0 and B_irr (for $B > B_{cr}$) in terms of these models.

Another problem encountered with using Eq. (4), which describes our IL, is the unphysical divergence of $B_\mathrm{irr}(T_\mathrm{irr} \to 0)$. Therefore, we expect that, at fields higher than those we used, B_irr will converge to some finite value, at least for $T = 0$. One of the observed dependencies, which avoids such divergence of the IL for $T_\mathrm{irr} \to 0$, is the exponential one,

$$B_\mathrm{irr}(T_\mathrm{irr}) = B^* \exp(-T_\mathrm{irr}/T_E) \tag{6}$$

which is reported in Bi2212 [33] and $HgBa_2CuO_{4+\delta}$ single crystals [19]. Unfortunately, there is no unique explanation [2,34–37] of the IL variation according to Eq. (6) and, furthermore, this equation cannot describe the observed B_irr data over an extended temperature range [38] with unique values of B^* and T_E. Indeed, our data for IL follow such dependence for 45 K< T_irr <65 K with $T_E = (14.5 \pm 0.5)$ K and $B^* = (80 \pm 10)$ T, but at lower temperatures, T_E gradually decreases and B^* increases, showing the inadequacy of such fit. Because of this, and because of different temperature variations of IL observed at low temperatures in several HTS compounds [7, 39] (similar to our one), we discuss below a model which is not based on 3D flux lines and provides $B_\mathrm{irr}(T = 0) = B_{c2}(0)$ as should be expected.

Kim and coworkers [4] suggest that $B_\mathrm{irr}(T)$ depends on two relevant energies. The first energy is the Josephson coupling energy E_{cj} for the phase of the superconducting order parameter [40, 41] between adjacent Cu–O multilayers

$$E_{cj} = \frac{\pi\hbar\Delta(T)}{2e^2 R_N} \tanh\frac{\Delta(T)}{2k_\mathrm{B}T}\left(1 - \frac{B}{B_{c2}(T)}\right) \tag{7}$$

where $\Delta(T)$ is the energy gap, and $R_N = \rho_c s B/\Phi_0$ is the normal-state resistance of the junction (ρ_c is c-axis resistivity and s is repeat distance of the Cu–O multilayers). The characteristic crossover temperature from 3D to 2D vortices is, therefore,

defined as $k_{\mathrm{B}}T = 2E_{cj}(B,T)$ (factor 2 accounts for both Cu–O bilayers). The second energy E_p is associated with the depinning of 2D pancake vortices within their Cu–O bilayer [42]

$$E_p = \alpha\pi\xi_{ab}^2 d_s \frac{B_c^2(T)}{2\mu_0}\left(1 - \frac{B}{B_{c2}(T)}\right)^2 \tag{8}$$

where α represents the effective strength of the pinning, ξ_{ab} is the coherence length in a–b plane and d_s is the thickness of closely coupled Cu-O planes in the multilayer. Characteristic depinning temperature is therefore defined as $k_{\mathrm{B}}T = E_p(B,T)$.

In order to move in transport measurements, vortices must overcome both energies, so in order to deduce relevant parameters, we solve the equation

$$k_{\mathrm{B}}T = 2E_{cj}(B,T) + E_p(B,T) \tag{9}$$

by fitting our $B_{\mathrm{irr}}(T_{\mathrm{irr}})$ data for $f = 10^{-6}$ to it using three fitting parameters: $B_{c2}(0)$, ρ_c and $B_c(0)$. Using the assumption from Ref. [4] that $\Delta(T)$ equals its BCS value $\Delta(T \to 0) = 1.76\ k_{\mathrm{B}}T_c$, $B_c(T)$ and $B_{c2}(T)$ take the clean-limit temperature dependence of $1 - t^2$ ($t = T/T_c$), $\xi_{ab}^2(T) = \xi_{ab}^2(0)/(1-t)$ and $\alpha = 1$, and structural data for Bi2223 compounds ($d_s = 0.32$ nm, $s = 1.352$ nm) and $T_c = 108$ K, obtained the fitting parameters are given in Table 2, together with other parameters which can be calculated from them. The resulting fit shows a good agreement with experimental data for $B \geq 2$ T, but deviates for lower fields, which can be explained by a stronger dependence of $\Delta(T)$ at high temperatures and by the fact that Eq. (9) does not describe vortex *line* interactions (which are in 3D regime, therefore applicable at low fields). The obtained superconducting parameters for Bi2223 compound (Table 2) are very reasonable and agree well with the available literature data. We obtained a similarly good agreement of the resistive $B_{\mathrm{irr}}(T_{\mathrm{irr}})$ data and Eq. (9) for a Bi2212 single crystal [7] measured in fields up to 50 T (Fig. 4).

TABLE 2. Values of the parameters obtained by fitting our $B_{\mathrm{irr}}(T_{\mathrm{irr}}, f = 10^{-6}\rho_n)$ data to Eq. (9): $B_{c2}(0)$ is the upper critical field, $B_c(0)$ is the thermodynamical critical field, $B_{c1}(0)$ is the lower critical field (all critical fields are at $T = 0$ K). Other quantities are calculated from these critical fields: κ is Ginzburg-Landau parameter, ρ_c is c–axis resistivity, $\xi_{ab}(0)$ and $\lambda_{ab}(0)$ are coherence length and penetration depth at $T = 0$ K in $a - b$ plane, respectively.

$B_{c2}(0)$ T	$B_c(0)$ T	$B_{c1}(0)$ mT	κ	ρ_c Ωcm	$\xi_{ab}(0)$ nm	$\lambda_{ab}(0)$ nm
115±10	0.57±0.01	14±1	143±13	6.8±0.5	1.69±0.07	242±23

An unusual low-temperature upturn of the resistive critical fields has recently been observed in single layer cuprates Bi2201, Tl2201 and 2D organic superconductors [39]. In Ref. [39], it was suggested that these upturns could be understood in terms of a simple approach based on thermodynamic fluctuations. The condition that the free energy in a coherence volume $\xi_{ab}(0)^2 d$ is approximately $k_{\mathrm{B}}T$, where

$\xi_{ab}(0)$ is the in plane coherence length and d is the interplane spacing, leads to the equation

$$B^*(T) = B_{c2}(0)\left(1 - \sqrt{T/T_0}\right) \tag{10}$$

as $T \to 0$. The present data do not extend down to such low temperatures as in Ref. [39], but from the fit of our $B_{\rm irr}(T_{\rm irr})$ data at the lowest temperature to Eq. (10), approximate values $B_{c2}(0) \approx 94$ T and T_0=36 K can be obtained. Hence $\xi_{ab}(0) \approx 1.9$ nm. The condensation energy or the thermodynamic critical field $B_c(0)$ of Bi2223 is not known as precisely as for YBCO due to a lack of the electronic specific heat measurements. Using the formula for T_0 in Ref. [39] (with $\alpha = 1$) leads to $B_c(0) = 0.5$ T. We will use this value in further discussion, but obviously further studies of this part are required. The corresponding κ value is 130 - typical of high T_c cuprates. With this value of B_c, it is interesting to evaluate the free energy in the field-dependent volume $\xi_{ab}(0)d\sqrt{\Phi_0/B}$. For $B = 1$ T, this corresponds to an activation energy proportional to $1/\sqrt{B}$ and equal to 900 K at 1 T. The experimental value is 2000 K at 1 T - which would require $B_c(0) = 0.8$ T instead of the above value. Taking into account a limited amount of $B_{\rm irr}(T_{\rm irr})$ data used in our fit (and the lack of data for $T \to 0$), we can conclude that a thermodynamic fluctuation model of the type described in Ref. [39] gives a reasonable quantitative description of the $B_{\rm irr}(T)$ behaviour observed at low T. More important, it provides another way of understanding the magnitude of the activation energy. In this picture it would be determined by the activation energy for normal regions, i.e. phase fluctuations in the coherence volume $\xi_{ab}(0)d\sqrt{\Phi_0/B}$. This model also shows the way to increase U^* and B^* in a given material. Since $B_c(0)$ falls strongly in the underdoped cuprates, with proper doping it might be possible to increase $B_c(0)$ of Bi2223 compound to 1.1 T (the value for $YBa_2Cu_3O_7$) in which case the activation energies could be as large as 4000 K at 1 T. Further, the parameter T_0 should also increase giving a larger value of $B_{\rm irr}$ at low T. Finally, we note that magnetically measured low-temperature variation of $B_{\rm irr}(T)$ for one Bi2212 single crystal [38] fits rather better Eq. (10) than Eq. (6). This may provide further support to the above model and its applicability to the Bi-Sr-Ca-Cu-O compounds.

5. *Conclusions*

From the low-resistivity parts of the resistive transitions on a Bi2223/Ag sheathed tape in magnetic fields B up to 15 T, we deduced effective activation energies $U(T, B)$. An analysis of the linear parts in the $\log\rho$ vs. $1/T$ plots shows that the resistivity onsets can be described by an effective activation energy $U(T, B) = U^*(1 - T/T_{\rm cs})/B^{0.5}$ throughout the explored field range. U^* is a sample-dependent constant, which, compared to the values for other types of Bi2223 samples, has a somewhat higher value. Such a dependence of $U(T, B)$ can be attributed to a thermally activated plastic deformation of 3D vortices in the pinned vortex-liquid regime of the $B-T$ phase diagram. However, in our field range ($B > B_{cr}$), 2D flux pancakes seem more likely than 3D vortices. Experimentally

obtained resistive irreversibility line IL, defined with the lowest accessible constant resistivity (0.2 nΩcm), follows from the observed form of $U(T, B)$, and throughout the explored range of B it obeys a power-law dependence $B_{\rm irr}(T_{\rm irr}) \propto (T_{\rm cs}/T_{\rm irr} - 1)^2$. Such a dependence throughout the explored field and temperature range is rather surprising, at least for low temperatures ($\approx$ 20 K) but it has been observed in a variety of Bi2223 and Bi2212 samples up to 18 T. Obviously, this dependence of $B_{\rm irr}$ cannot extend down to $T = 0$. Another observed variation of IL in Bi-Sr-Ca-Cu-O superconductors is the exponential one, $B_{\rm irr}(T_{\rm irr}) \propto \exp(-T_{\rm irr}/T_E)$, which can arise from several mechanisms and is free from divergence of $B_{\rm irr}(T = 0)$, but this dependence does not lead to a unique value of T_E when $B_{\rm irr}$ is measured over a broad temperature range (as in our case). Because of the difficulties with IL variations discussed above, we have analyzed our $B_{\rm irr}$–$T_{\rm irr}$ data in terms of two models which predict rapid increase of $B_{\rm irr}$ as $T \to 0$ (as observed), but also yield a plausible result $B_{\rm irr}(T = 0) = B_{c2}(0)$.

Our data for $B_{\rm irr} \geq 2$ T fit well the expression for IL (Eq. (9)) derived by Kim et al. [35] (which associates IL with the competition of the interlayer decoupling and intralayer depinning of vortices) and the parameters of the fit yield very reasonable values for superconducting parameters of Bi2223 compound (Table 2). In order to analyze the applicability of this expression at even lower $T_{\rm irr}$ (higher $B_{\rm irr}$), we have also analyzed recent results for IL of a Bi2212 single crystal [7] (measured up to 50 T) and found a similarly good fit (Fig. 4) and sound values for the superconducting parameters of the Bi2212 compound. Finally, we have also checked the applicability of the expression (Eq. (10)) proposed in Ref. [39] for the explanation of the low-temperature upturns in the critical fields of single-layer cuprates (Bi2201, Tl2201) to our $B_{\rm irr}(T_{\rm irr})$ data for the lowest measured temperatures. Considering the limited amount of data points employed and the lack of data for $T \to 0$, this fit also yields reasonable $B_{c2}(0)$, ξ_{ab}, $B_c(0)$ and κ for the Bi2223 compound. Therefore, there seem to be at least two models which may be able to explain the IL of Bi-Sr-Ca-Cu-O superconductors at the lowest temperatures. Clearly, accurate measurements of IL at very low temperatures are required in order to single out which model describes best the nature of IL for $T \to 0$.

References

1) See for example Y. B. Kim and M. J. Stephen, *Superconductivity*, ed. R. D. Parks, Marcel Dekker, New York (1969) p. 1107;

2) G. Blatter, M. V. Feigel'man, V. B. Geshkenbein, A. I. Larkin and V. M. Vinokur, Rev. Mod. Phys. **66** (1994) 1125;

3) T. T. M. Palstra, B. Batlogg, L. F. Schneemeyer and J. V. Waszczak, Phys. Rev. B **43** (1991) 3756;

4) D. H. Kim, K. E. Gray, R. T. Kampwirth, J. C. Smith, D. S. Richeson, T. J. Marks, J. H. Kang, J. Talvacchio and M. Eddy, Physica C **177** (1991) 431;

5) J. R. Clem, Phys. Rev. B **43** (1991) 7837;

6) L. Civale, Supercond. Sci. Technol. **10** (1997) A11;

7) Y. Ando et al., Phys. Rev. B **60** (1999) 12475;

8) W. G. Wang, P. A. Bain, J. Horvat, B. Zeimetz, Y.C. Guo, H.K. Liu and S.X. Dou, Supercond. Sci. Technol. **9** (1996) 881;

9) I. Kušević, P. Šimundić, J. Ivkov, E. Babić, W. G. Wang, H. K. Liu and S. X. Dou, Physica C **282-287** (1997) 2297;

10) E. Babić, I. Kušević, S. X. Dou, H. K. Liu and Q.Y. Hu, Phys. Rev. B **49** (1994) 15312;

11) P. Wagner, U. Frey, F. Hilmer and H. Adrian, Phys. Rev. B **51** (1995) 1206;

12) H. Yamasaki, K. Endo, S. Kosaka, M. Umeda, S. Yoshida and K. Kajimura, Phys. Rev. B **49** (1994) 6913;

13) E. Babić, I. Kušević, K. Zadro, J. Ivkov, Ž. Marohnić, Đ. Drobac, M. Prester, H. K. Liu, S. X. Dou, D. Todorović-Marinić and A. Kuršumović, Fizika A (Zagreb) **4** (1995) 549;

14) Y. Iwasa, E. J. McNiff, R.H. Bellis and K. Sato, Cryogenics **33** (1993) 836;

15) J. T. Kucera, T. P. Orlando, G. Virshup and J. N. Eckstein, Phys. Rev. B **46** (1992) 11004;

16) R. G. Beck et al., Phys. Rev. Lett. **68** (1992) 1594;

17) H. Safar et al., Phys. Rev. Lett. **69** (1992) 824; **70** (1993) 3800;

18) W. K. Kwok et al., Phys. Rev. Lett. **69** (1992) 3370; **72** (1992) 1088; **72** (1992) 1092;

19) M. Pissas, E. Moraitakis, G. Kallias, A. Terzis, D. Niarchos and M. Charalambous, Phys. Rev. B **58** (1998) 9536;

20) A. Schilling, R. Jin, J. D. Guo and H. R. Ott, Phys. Rev. Lett. **71** (1993) 1899;

21) L. I. Glazman and A. E. Koshelev, Phys. Rev. B **43** (1991) 2835;

22) M. V. Feigel'man, V. B. Geshkenbein and A. I. Larkin, Physica C **167** (1990) 177;

23) Y. Mawatari, H. Yamasaki, S. Kosaka and M. Umeda, Cryogenics **35** (1995) 161;

24) I. Kušević, E. Babić, Ž. Marohnić, J. Ivkov, H. K. Liu and S. X. Dou, Physica C **235-240** (1994) 3035;

25) V. B. Geshkenbein, M. V. Feigel'man, A. I. Larkin and V. M. Vinokur, Physica C **162-164** (1989) 239;

26) P. Wagner, F. Hilmer, U. Frey and H. Adrian, Phys. Rev. B **49** (1994) 13184;

27) T. Tsuboi, T. Hanaguri and A. Maeda, Phys. Rev. B **55** (1997) R8709;

28) J. H. Cho, M. P. Maley, S. Fleshler, A. Lacerda and L. N. Bulaevskii, Phys. Rev. B **50** (1994) 6493;

29) I. Matsubara, H. Tanigawa, T. Ogura, H. Yamashita and M. Kinoshita, Phys. Rev. B **45** (1992) 7414;

30) D. López, L. Krusin-Elbaum, H. Safar, E. Righi, F. de la Cruz, S. Grigera, C. Feild, W. K. Kwok, L. Paulius and G. W. Crabtree, Phys. Rev. Lett. **80** (1998) 1070;

31) Y. Abulafia, A. Shaulov, Y. Wolfus, R. Prozorov, L. Burlachkov and Y. Yeshurun, Phys. Rev. Lett. **77** (1996) 1596;

32) A. V. Bondarenko, V. A. Shklovskij, M. A. Obolenskii, R. V. Vovk, A. A. Prodan, M. Pissas, D. Niarchos and G. Kallias, Phys. Rev. B **58** (1998) 2445;

33) M. V. Indenbom, G. D'Anna, M.-O. André, W. Benoit, H. Kronműller, T. W. Li and P. H. Kes, *Proc. 7th Int. Workshop on Critical Currents in Superconductors*, ed. H. W. Weber, World Scientific, Singapore (1994) p. 327;

34) A. E. Koshelev and V. M. Vinokur, Physica C **173** (1991) 465;

35) K. E. Gray, D. H. Kim, B. W. Veal, G. T. Seidler, T. F. Rosenbaum and D. E. Farell, Phys. Rev. B **45** (1992) 10071;

36) P. de Rango, B. Giordanengo, R. Tournier, A. Sulpice, J. Chaussy, G. Deutscher, J. L. Genicon, P. Lejay, R. Retoux and B. Raveu, J. Phys. (France) **50** (1989) 2857;

37) L. Burlachkov et al., Phys. Rev. B **50** (1994) 16770;

38) C. D. Dewhurst, D. A. Cardwell, A. M. Campbell, R. A. Doyle, G. Balakrishnan and D. K. McK Paul, Phys. Rev. B **53** (1996) 14594;

39) J. R. Cooper, J. W. Loram and J. M. Wade, Phys. Rev. B **51** (1995) 6179, and references therein;

40) V. Ambegaokar and A. Baratoff, Phys. Rev. Lett. **10** (1963) 486;

41) D. H. Kim, K. E. Gray, R. T. Kampwirth, K. C. Woo, D. M. McKay and J. Stein, Phys. Rev. B **41** (1990) 11642;

42) K. E. Gray. R. T. Kampwirth, J. M. Murduck and D. W. Capone II, Physica C **152** (1988) 445.

GRANICA IREVERZIBILNOSTI VRPCE Bi2223/Ag U SNAŽNIM MAGNETSKIM POLJIMA

Mjerili smo magnetootpor $(Bi,Pb)_2Sr_2Ca_2Cu_3O_{10+y}$ vrpce obložene srebrom za temperature 15 K $\leq T \leq$ 120 K i u magnetskim poljima $B \leq 15$ T okomitim na širu plohu vrpce. U svim poljima početak otpora pokazuje Arrheniusovo ponašanje $\rho \propto \exp(-U^*(1 - T/T_{cs})/k_B T B^{0.5})$, gdje je U^* konstanta ovisna o uzorku, a T_{cs} je temperatura nešto viša od temperature pojave otpora. Primijetili smo da se ovisnost otpornosti može pripisati termički pobuđenom tečenju toka u jako viskoznom području tekućine magnetskih vrtloga karakteriziranom plastičnim deformacijama magnetskih vrtloga. Eksperimentalno određena otporna linija ireverzibilnosti $B_{irr}(T_{irr})$ slijedi potencijsku ovisnost $B_{irr}(T_{irr}) \propto (T_{cs}/T_{irr} - 1)^2$ koja se može izvesti iz eksponencijalnoe ovisnosti otpornosti. Naši $B_{irr}(T_{irr})$ podaci isto tako mogu se prilagoditi modelu Josephsonovog vezanja i otpinjanja magnetskih vrtloga–palačinki. Ova prilagodba daje razumne vrijednosti parametara B_{c2}, B_{c1}, B_c, ξ_{ab} i λ_{ab} Bi2223 spoja, te uklanja nefizikalnu divergenciju $B_{irr}(T \to 0)$ koja se dobiva iz potencijske ovisnosti.